



Particle formation on the YBCO thin film surface: effect of stoichiometry and substrate material

P.B. Mozhaev^{a,b,*}, F. Rönning^a, P.V. Komissinskii^{a,b}, Z.G. Ivanov^a,
G.A. Ovsyannikov^b

^a Chalmers University of Technology, Department of Microelectronics and Nanoscience, SE-41296, Göteborg, Sweden

^b Institute of Radio Engineering and Electronics, Russian Academy of Sciences, Mokhovaya Str. 11, 103907, Moscow, Russia

Received 29 November 1999; accepted 29 February 2000

Abstract

Particle formation on the $\text{YBa}_2\text{Cu}_3\text{O}_{7-x}$ (YBCO) thin film surface deposited by laser ablation was studied. Ablation of a stoichiometric YBCO target results in Ba-deficient films, probably due to Ba scattering in oxygen atmosphere. Partial melting of the target surface during ablation provided additional Ba flow and resulted in smooth films. Surface quality of the YBCO film with improved element composition depends on lattice mismatch between the growing film and the substrate. Increase of deposition temperature over some threshold level, specific for each tested substrate material, results in particle appearance on the film surface even in the films with improved element composition. Chemical interaction, caused by oxygen depletion of the substrate surface, can be the reason for this effect. © 2000 Elsevier Science B.V. All rights reserved.

PACS: 68.55. – a; 74.76.Bz; 81.15.Fg

Keywords: YBCO thin films; Precipitates; Chemical interaction with substrate

1. Introduction

Particle formation on the $\text{YBa}_2\text{Cu}_3\text{O}_{7-x}$ (YBCO) thin film surface seriously limits the application of these superconducting films. A huge amount of papers was published on this topic, see, e.g. Refs. [1–5]. Two reasons for the particle formation are generally stated. Partial decomposition of the film when the deposition conditions are far from optimal conditions of YBCO formation provides grains of

individual oxides and decreases superconducting quality of the film. Local or overall non-stoichiometry of the film results in extraction of the excess material into particles of non-superconducting oxide phases. Excess Y is often incorporated into the YBCO film as Y_2O_3 inclusions while CuO , Y_2BaCuO_5 , and different barium–copper oxides are usually observed as precipitates on the YBCO film surface [1–5].

Another type of particles often observed on the YBCO film surface are particles of YBCO of different orientations, i.e. (100)-oriented (*a*-oriented) inclusions in (001)-oriented (*c*-oriented) films and *c*-oriented inclusions in *a*-oriented films. Formation of these inclusions is controlled by kinetic factors, leading in general to *a*-oriented film growth at low deposition temperatures and *c*-oriented film growth

* Corresponding author. Institute of Radio Engineering and Electronics RAS, Mokhovaya Str. 11, 103907, Moscow, Russia. Tel.: +7-95-203-0935; fax: +7-95-203-8414.

E-mail address: pbmzh@hitech.cplire.ru (P.B. Mozhaev).

at high deposition temperatures [6,7]. In some cases, though, formation of *a*-oriented inclusions is caused by chemical interaction between the substrate and the deposited material in the very beginning of deposition. The products of such a reaction suppress epitaxial growth in their vicinity resulting in *a*-oriented particle seeding even at high deposition temperatures [8,9].

Laser ablation is one of the most often used techniques for production of high-quality YBCO thin films. The ablation process results in conservation of the target stoichiometry in the initially ablated cloud, but scattering processes during the material propagation can result in deviations from stoichiometry both on the axis of the propagating material (plume) and in the off-axis regions [10,11].

In the present paper, we study the particle seeding on the surface of the YBCO thin film deposited by laser ablation. Different methods of particle formation suppression are suggested, and the effect of substrate material on the particle formation at different temperatures is investigated.

2. Experimental

The laser deposition system was described in detail in Ref. [12]. In short, the KrF excimer laser provided an energy density on the target of up to 3 J/cm² with a pulse duration less than 30 ns. A one-lens spot formation optical system allowed the change of spot size and spot position on the target. Two spot positions were used (Fig. 1): “donut” position I, covering a donut area during target rotation and thus improving the lifetime of the target, and “centred” position II with overlapping of spots

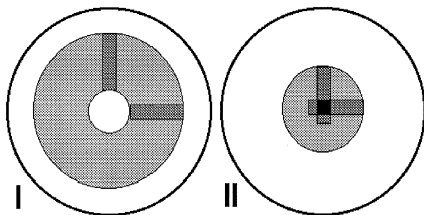


Fig. 1. Two possible positions of the laser beam on the target and areas, covered on the target during rotation. Sequential spots overlap in the target centre for position II.

in the target centre. The deposition pressure in the chamber was set in the 0.05–1 mbar range by adjustment of the oxygen flow at constant pumping rate of the evacuation system. The ThermoCoax heating element provided heating of the sample holder up to 850°C. The desired temperature and heating rate were controlled by a EuroTherm controller. The substrate was glued on the holder with silver paint, providing good thermal contact. The target–substrate distance was about 60 mm. Standard deposition conditions were: substrate temperature, 750–800°C; oxygen pressure, 0.8 mbar; laser beam energy density on the target, 1.7 J/cm²; repetition rate, 10 pulses/s; resulting in deposition rate about 0.6 Å/pulse. The visible plume length at standard deposition conditions was about 45 mm, placing the substrate out of the plume. After deposition, the chamber was filled with oxygen to 900 mbar pressure and the samples were left at 400–450°C for 1 h providing necessary oxidation of the YBCO film.

The superconducting properties of the deposited films were determined by measuring the magnetic susceptibility dependence on temperature. The critical temperature T_c was determined as the highest temperature at which the screening effect was observed. The width of the superconducting transition ΔT_c , showing the degree of uniformity of the superconducting properties of the film, was measured between 10% and 90% levels of the maximal screening effect. The structure of the films was investigated using X-ray diffractational $\theta/2\theta$ -scans, providing information on phase composition and lattice parameters. Precise calculations of the interplanar distance were done using all available peaks [13]. The dependence of the $\theta/2\theta$ -scan peak width on 2θ was analysed to evaluate strain in the studied films [5]. Element composition of some films was studied using X-ray microanalysis. The electron beam scanned over a $100 \times 100 \mu\text{m}^2$, providing overall element composition of the film and particles on its surface. Film surface quality was characterised by two parameters: density of particles and surface roughness. The density of particles was determined using optical microscope, so only particles greater than $0.5 \mu\text{m}$ in size were taken into account for this calculation. The roughness parameter R_a (mean square of vertical distances between neighbour peak and valley) was determined using profile meter. The

scan velocity was 2 $\mu\text{m/s}$, vertical accuracy was 5 \AA , and scan distance was 50 μm .

3. Results and discussion

3.1. Donut spot position

The YBCO films deposited at standard deposition conditions on the LaAlO_3 (001) substrates showed T_c of 88–90°C and ΔT_c less than 1.5 K; the critical current density at 77 K exceeded 10^6 A/cm^2 . The X-ray investigations showed that the films were completely c-oriented with c lattice constant about 11.7 \AA and strain along substrate normal less than 0.5% (see Table 1). No additional phase peaks were observed. The optical micrographs of typical YBCO films, deposited from a stoichiometric YBCO target, are shown in Fig. 2. The density of particles on the film surface varies from 5×10^6 to 10^8 cm^{-2} . A typical particle is shown on the upper-left inset of Fig. 2c; clear facets with hexagonal symmetry are observed. A precise tuning of the geometrical factors of deposition, such as target–substrate distance, substrate shift from the plume axis, laser beam energy density on the target and deposition pressure, decreases the particle density to 10^6 cm^{-2} , but even a slight change in the stated deposition conditions results in a rapid increase of particle density. Good superconducting properties of the deposited films imply deposition conditions close to the optimal for the YBCO film formation excluding particle formation due to decomposition of the film. This supposition is confirmed also by low ($< 0.5\%$) strain of the films (Table 1). The particle formation, hence, takes place mainly due to composition deviations from stoichiometric metal ratio 1:2:3. Comparison of the element composition of laser deposited films with

that of films deposited by DC-sputtering at high pressure [14] showed 5–8% Ba-deficiency in the laser deposited films. Evaluation of the particle volume ratio to the overall film volume gives close numbers (Table 1). Deposition at standard parameters from a target with excess Ba ($\text{Y}_1\text{Ba}_{2.2}\text{Cu}_3\text{O}_x$) resulted in a smooth film with particle density less than $2 \times 10^6 \text{ cm}^{-2}$ without special deposition parameter tuning. T_c of the obtained films was about 88.5 K and ΔT_c was less than 2.0 K. Ba-deficiency is often observed type of YBCO film non-stoichiometry, resulting in copper-rich particles on the film surface. Excess Y is incorporated into the film as Y_2O_3 inclusions and cannot be seen in SEM or optics [3]. The hexagonal shape of particles (inset of Fig. 2c) can be produced by a (111)-oriented phase with cubic lattice, like CuO. The X-ray $\theta/2\theta$ -scans showed some diffraction intensity increase at CuO (111) peak position (38.73°), but close vicinity of a strong (005) YBCO peak makes impossible clear peak observation. Two possible reasons for Ba-deficiency in the films deposited from stoichiometric YBCO targets can be suggested: Ba scattering in oxygen atmosphere and Ba re-evaporation from the growing film. Strong dependence of the particle density on geometrical factors suggests that scattering is the main cause.

Both particle size and density depend on the deposition temperature (Fig. 2, Table 1). At deposition temperatures less than 760°C, particles of 0.7–1.2 μm size were observed with densities $(5\text{--}10) \times 10^6 \text{ cm}^{-2}$, while at temperatures higher than 770°C, typical particles were 0.5–0.8 μm in diameter and their density was up to 10^8 cm^{-2} . At 765°C, both types of particles could be observed, supposing presence of two different seeding mechanisms. Evaluation of the particle volume gives the same factors for

Table 1

Properties of the YBCO thin films deposited on LaAlO_3 (001) substrates by laser ablation with donut spot position, and parameters of numerical simulation of particle seeding

Deposition temperature (°C)	C lattice constant (\AA)	Strain (%)	Average particle size (μm)	Average distance between particles (μm)	Particles volume (% of the film volume)	Simulation parameters		
						Excess material (%)	Diffusion length (μm)	Stoichiometry fluctuations (%)
750	11.714	0.18	0.95	6	6.9	5	4.5	5
765	11.698	0.12	1.1	8	6.6	5	10	5
780	11.702	0.31	0.75	1.5	6.5	5	32	5

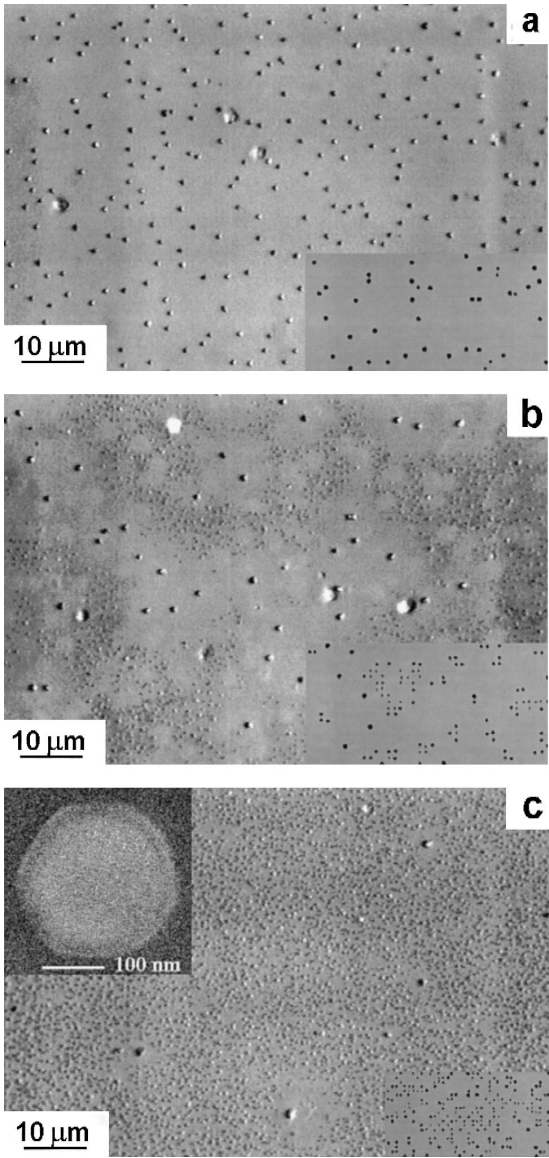


Fig. 2. Micrographs of YBCO thin films deposited on LaAlO_3 (001) substrates from a stoichiometric $\text{YBa}_2\text{Cu}_3\text{O}_{7-x}$ target using laser ablation with donut laser beam spot position. Substrate temperature: (a) 750°C; (b) 765°C; (c) 780°C. On the right-bottom insets: simulated particle pattern, simulation parameters in Table 1. On the upper-left inset (c): SEM micrograph of a typical particle.

all deposition temperatures, proving the same level of overall non-stoichiometry at all deposition temperatures. Strong dependence of Ba re-evaporation

rate on temperature excludes re-evaporation as possible reason for the film overall non-stoichiometry.

We performed computer simulations of the particle seeding with the following suppositions: (i) only excess material is incorporated into particles; (ii) excess material amount fluctuates along the surface; (iii) seeding of a particle becomes possible when one monolayer of excess material (e.g. CuO) is present on the film surface. Seeding probability was set to 1/2 for simplicity. Excess material is added at moments t_N (laser pulses)

$$c(x, t > t_N) = c(x, t_N) + c_p(1 + k\xi), \quad (1)$$

where $c(x, t)$ is excess material amount on the film surface, c_p is the excess material amount in the plume, k is the fluctuations intensity, and ξ is a stochastic variable uniformly distributed in $[-1/2, 1/2]$. If the particle was seeded in some point x_p on the surface, the excess material around the particle is supposed completely consumed: $c(x_p, t > t_N) = 0$. The excess material distribution between the pulses was “smoothened” by diffusion

$$\partial c / \partial t = -D \partial^2 c / (\partial x)^2, \quad (2)$$

where $D = l_d^2 / \tau$ is the diffusion constant: l_d is the characteristic diffusion length and τ is the characteristic diffusion time. Diffusion “smoothening” makes seeding of the particles possible only immediately after laser pulse; additional surface fluctuations of the excess material were not taken into account. The simulation parameters were chosen using the observed particle patterns: c_p should be approximately the observed volume of particles relative to the overall film volume and l_d should be close to the observed distance between big particles (Table 1). To obtain necessary l_d numerically, the time scale of the simulation (number of smoothing steps between pulses) was changed. Characteristic diffusion time τ was chosen as time of diffusion transport of material from the target to the substrate being about 0.01 s [15]. Fluctuation intensity k was used as tuning parameter. One-dimensional test simulations were performed first and after that Eqs. (1) and (2) were generalised for the two-dimensional case. The simulated patterns similar to the observed ones are shown in the bottom-right corners of Fig. 2 and the simulation parameters used are stated in Table 1.

Possible reason for particle seeding at low deposition temperatures is fluctuation of the element distribution on the substrate surface. The threshold amount of excess material is accumulated on the film surface during some initial period (Fig. 3 inset, 75–90 laser pulses). After seeding the growing particle acts as a sink for excess material, suppressing seeding of new particles in its vicinity (Fig. 3 inset, 95–110 laser pulses). Far from the particle, new seeding still can occur, prolonging the period of particle seeding (Fig. 3, dotted line). The resulting particles are big and sparse; the particle size depends on the distance to the neighbour particles. Experimental investigations of particle seeding on the early stages of YBCO film formation showed no particles on the film surface (see, e.g. Ref [16]). The particles appear during a short period of deposition and suppress further seeding [16]. These observations are in good agreement with suggested simple particle seeding model.

“Fluctuational” seeding mechanism explains YBCO film surface morphology at low deposition temperatures, with increase of particle size and distance between them with increase of deposition temperature. The small distance between particles at high deposition temperature (Fig. 2c) can be explained as sudden decrease of diffusion intensity

along the surface, for example, as a result of characteristic time increase, but presence of both dense and sparse particles at intermediate temperature (Fig. 2b) demands second seeding mechanism. Such a mechanism can be provided by an increase of diffusion at high deposition temperatures, making it sufficient to smoothen all fluctuations before a particle can be seeded due to fluctuation. In this case, the amount of excess material increases almost uniformly along the film surface and seeding of particles occurs in many places simultaneously (Fig. 3, solid line). The area per particle decreases, and the size of resulting particles is smaller than in the case of fluctuational seeding. Both mechanisms coincide at intermediate diffusion intensities, as can be seen on inset Fig. 2b, with fluctuational seeding on earlier stages of deposition and accumulative seeding on later stages (Fig. 3, dashed line).

3.2. Centred spot position

We found out that shifting the laser beam spot position to the centre of the stoichiometric YBCO target (position II, Fig. 1) results in a dramatic decrease of the particle density on the film surface to less than 10^6 cm^{-2} . This effect is observed for both

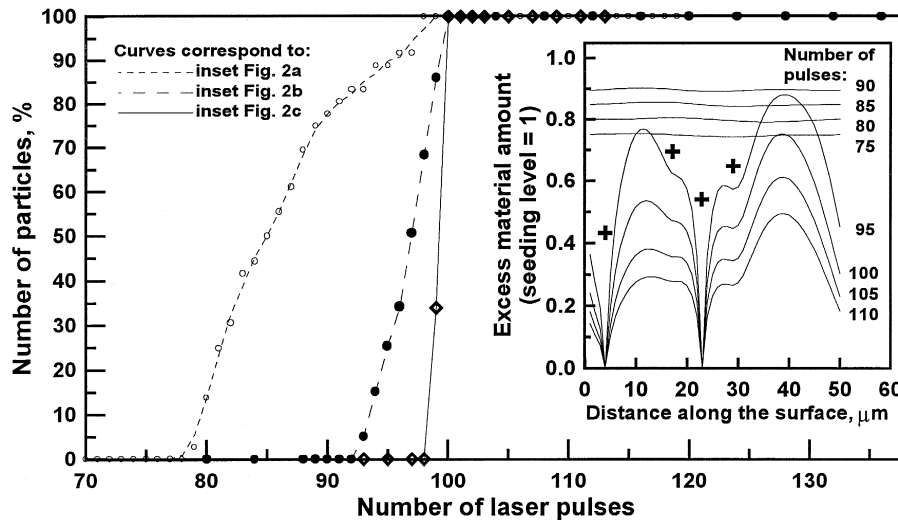


Fig. 3. Simulation of the particle seeding during deposition: increase of diffusion length decreases the seeding period. Lines correspond to insets Fig. 2a–c. On the inset: cross-section of the excess material distribution after 75–110 laser pulses, crosses mark positions of the particles seeded in vicinity of the presented cross-section. Simulation parameters same as on the Fig. 2b inset.

spot position crossing the centre of the target and for spots just overlapping in the centre. The shape and size of the plume do not differ significantly from the case of donut ablation. The central part of the target after ablation is partially molten in contrast to the outer regions (Fig. 4). The typical for laser ablation columnar hillocks on the target surface are tilted to the laser in case of donut ablation and normal to the target surface when the spot is centred. Melting of the target in the area of spot overlapping seems to be the reason for the improved surface quality of the film. The post-ablation Ba flow from the target surface was observed in Ref. [11]; possible reason for such additional Ba emission can be heating of the target by the ablated cloud. To test heating effect, we decreased the laser beam repetition rate two times resulting in increase of the particle density to $2 \times 10^6 \text{ cm}^{-2}$. Further decrease of the repetition rate restored the particle density to values typical for donut abla-

tion. The melting temperature of any combination of target elements is higher than 800°C [17]. Ba evaporation rate at these temperatures is very high, so one can suppose additional Ba flow from the molten parts of the target, compensating Ba deficiency due to scattering.

Using the centre ablation technique, we studied deposition of smooth YBCO films on different substrates in temperature range $760\text{--}820^\circ\text{C}$. The deposition was performed simultaneously on four substrates: (001) LaAlO_3 , (110) NdGaO_3 , (001) SrTiO_3 , and (001) CeO_2 -buffered (1102) sapphire. The YBCO film parameters at deposition temperature 780°C are given in Table 2. The surface smoothness depends strongly on the lattice mismatch between the growing film and substrate (Fig. 5): both density of particles and roughness of the film monotonously increase with the lattice mismatch for deposition temperatures less than 790°C . Lattice mismatch was calculated as $(d_F - d_S)/d_S \times 100\%$, where $d_F = (a^2 + b^2)^{1/2} = 5.454 \text{ \AA}$ is the [110] translation distance of YBCO and d_S is the corresponding translation distance of the substrate surface, namely [110] LaAlO_3 , [001] NdGaO_3 , [110] SrTiO_3 , and [100] CeO_2 , all taken at room temperature. Dependence of surface morphology on lattice mismatch, probably, results from prolonged layer-by-layer growth on the substrate with smaller lattice mismatch [18]. The superconducting parameters and crystal quality of the films show generally opposite behaviour: films on LaAlO_3 have highest critical temperature and lowest lattice strain compared with films on substrates with smaller lattice mismatch. Lattice strain of the YBCO films on LaAlO_3 substrates deposited using donut ablation is even smaller (see Table 1), supposing dependence of the film strain on particle density. More uniform oxygenation of the films along the particles [19,20] and strain relaxation at the particles sites can be the reasons for this effect.

With increase of deposition temperature over some threshold level, many small particles appear on the film surface (Fig. 6). The threshold level was about 790°C for CeO_2 -buffered sapphire and about 810°C for SrTiO_3 , LaAlO_3 , and NdGaO_3 . Formation of a-oriented particles is observed usually at temperatures $10\text{--}20^\circ\text{C}$ below threshold (see inset Fig. 6). Three possible reasons for particle formation at high deposition temperatures can be supposed: (i) devia-

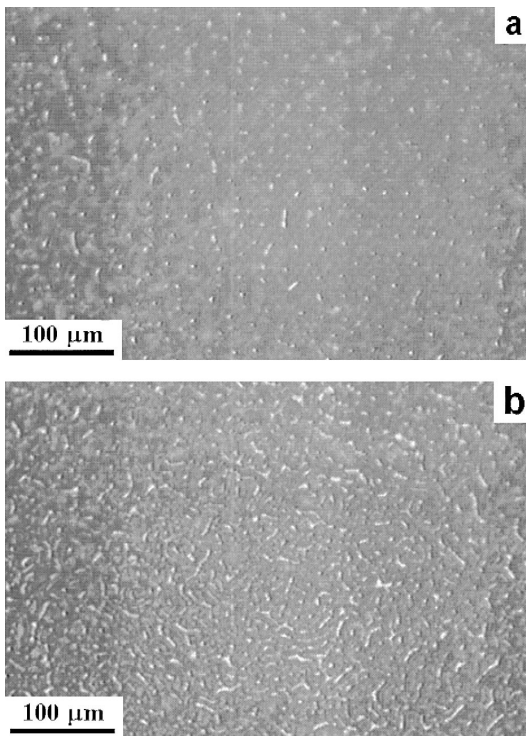


Fig. 4. Micrographs of the stoichiometric $\text{YBa}_2\text{Cu}_3\text{O}_{7-x}$ target after 770 laser shots with centred laser spot position: (a) outer region of the target; (b) central part of the target.

Table 2

Properties of the YBCO thin films, simultaneously deposited on different substrates by laser ablation with centred position of the spot at standard deposition conditions; deposition temperature 780°C

Parameter	Substrate			
	NGO(110)	CeO ₂ (001) Al ₂ O ₃ (1102)	STO(001)	LAO(001)
Critical temperature (K)	89.6	89.4	89.6	90.0
Superconducting transition width (K)	1.2	0.3	0.5	0.9
Surface roughness (Å)	25	30	40	100
Particle density on the film surface ($\times 10^5 \text{ cm}^{-2}$)	0.7	3	5	11
Lattice constant <i>c</i> (Å)	11.70	11.68	11.685	11.70
FWHM (005) (°)	0.24	0.17	0.22	0.2
Film strain (%)	0.8	0.6	0.75	0.6

tion from optimal YBCO formation conditions and partial decomposition of the film; (ii) Ba re-evaporation from the substrate resulting in overall non-stoichiometry of the film; (iii) chemical interaction with the substrate suppressing epitaxial film growth. Both superconducting properties and crystal quality of the deposited films improve with increase of temperature even after appearance of the particles (Fig. 7). This improvement implies close vicinity of the deposition conditions to the optimal conditions of YBCO formation and thus excludes partial decomposition of the film. On the other hand, if Ba re-evaporation is a

main reason for particle appearance, the threshold temperature should be the same for all studied substrates.

Chemical reactions of the deposited YBCO film with substrates were observed for many substrate materials [21–23]. *a*-oriented inclusions, as signs of chemical interaction, were observed for NdGaO₃ substrates [8,9]. Appearance of *a*-oriented particles at temperatures slightly lower than threshold deposition temperature allows supposition of the chemical nature of particle formation at high deposition temperatures. The reason for chemical interaction can be oxygen depletion of the substrate surface after heating to deposition temperature in vacuum [24]. We

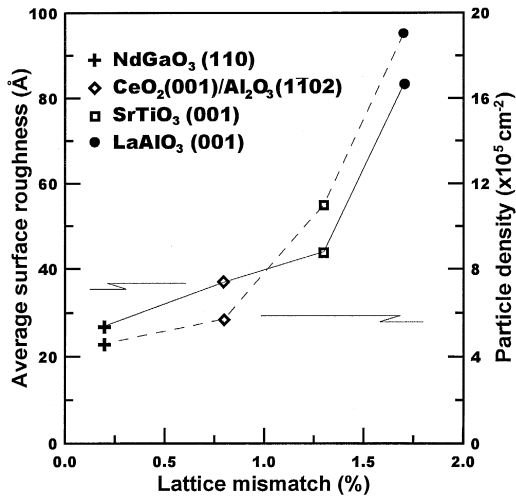


Fig. 5. Surface quality dependence on the lattice mismatch between the substrate and the YBCO thin film. The YBCO films on four different substrates were deposited simultaneously by laser ablation using the centred laser spot position, deposition temperature 780°C.

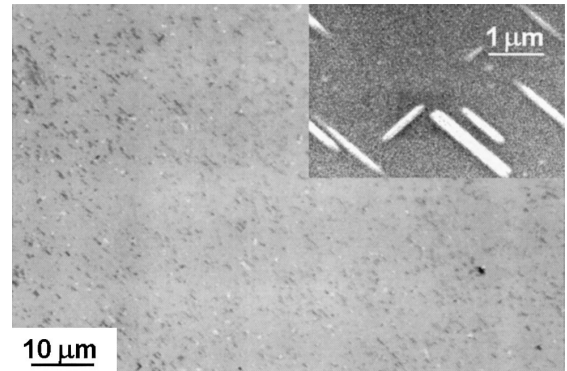


Fig. 6. Micrograph of the YBCO thin films deposited on NdGaO₃ (110) substrate using laser ablation of a stoichiometric YBa₂Cu₃O_{7-x} target with centred laser beam spot position, deposition temperature 820°C. On the inset: SEM micrograph of the *a*-orientated particles appearing with the increase of deposition temperature.

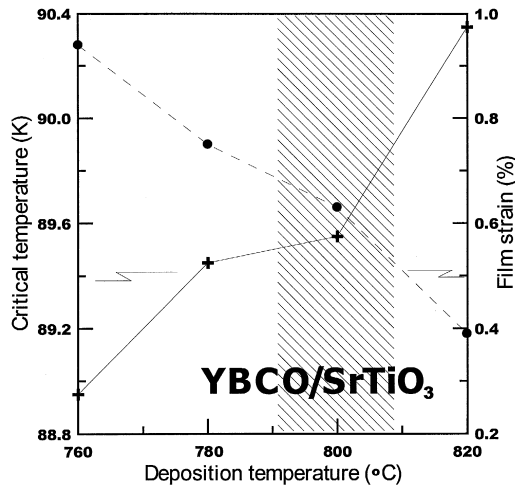


Fig. 7. Dependence of the YBCO thin film properties on the deposition temperature. Films deposited on SrTiO₃ (001) substrate by laser ablation with the centred spot position. The a-oriented particles appear on the film surface at about 790°C, precipitates observed at temperatures above 810°C.

deposited films on (001) SrTiO₃ and (001) LaAlO₃ substrates after leaving them for 30 min in vacuum at 780°C. The resulting films were polycrystalline and showed no superconductive transition. Even 10 min dwell of the substrate in vacuum at deposition temperature decreased critical temperature of the resulting film to 86–87 K. No effect of dwell at 760–780°C in 0.6 mbar oxygen was observed.

4. Conclusions

We studied particle formation on the YBCO thin film surface deposited by laser ablation technique. Films deposited by ablation of a stoichiometric YBCO target were Ba-deficient, probably due to Ba scattering in oxygen atmosphere. Partial melting of the target surface during ablation resulted in smooth films; Ba evaporation from molten parts can be the reason for this effect. Decrease of lattice mismatch between the growing film and the substrate improves smoothness of the film surface. Deposition of YBCO films at different temperatures showed the presence of a threshold temperature, specific for each substrate material. At a temperature higher than threshold, particles appear even in the films with improved

element composition. Chemical interaction due to oxygen depletion of the substrate surface can be the reason for particle formation at high deposition temperatures.

Acknowledgements

Authors would like to thank Dr. P. Larsson, Chalmers University of Technology, Gothenburg, Sweden, for the help in experiments, Dr. T. Claeson and Dr. D. Winkler, Chalmers University of Technology, Gothenburg, Sweden, for the useful discussion.

The work was supported in part by the ESPRIT contract, 23429 HTS-RSFQ, Swedish Material Consortium on superconductivity, Russian State Program “Modern Problems of the Solid State Physics”, “Superconductivity” division, Russian Foundation for Basic Research and INTAS program of EU.

References

- [1] S. Proyer, E. Stangl, M. Borz, B. Hellebrand, D. Bauerle, *Physica C* 257 (1996) 1.
- [2] D. Bhatt, *Physica C* 222 (1994) 283.
- [3] K. Verbist, A. Kuhle, A.L. Vasiliev, *Physica C* 269 (1996) 131.
- [4] M. Kawasaki, M. Nantoh, *MRS Bull.* XIX (9) (1994) 33.
- [5] J.P. Gong, M. Kawasaki, K. Fujito, R. Tsuchiya, M. Yoshimoto, H. Koinuma, *Phys. Rev. B* 50 (5) (1994) 3280.
- [6] F. Mileto Granozio, U. Scotti di Uccio, *J. Cryst. Growth* 175 (1997) .
- [7] U. Jeschke, R. Schneider, G. Ulmer, G. Linker, *Physica C* 243 (1995) 243.
- [8] Yu.A. Boikov, Z.G. Ivanov, E. Olsson, V.A. Danilov, T. Claeson, M. Shcheglov, D. Erts, *Phys. Solid State Fizika Tverdogo Tela* 37 (3) (1995) 880, in Russian.
- [9] P.B. Mozhaev, G.A. Ovsyannikov, S.N. Polyakov, E.K. Kov’ev, N.P. Kukhta, *Supercond.: Phys., Chem., Tech.* 9 (1996) 304, in Russian.
- [10] Z. Trajanovich, L. Senapati, R.P. Sharma, T. Venkatesan, *Appl. Phys. Lett.* 66 (18) (1995) 2418.
- [11] Y. Nakata, W.K.A. Kumuduni, T. Okada, M. Maeda, *Appl. Phys. Lett.* 66 (23) (1995) 3206.
- [12] P. Larsson, Sub-micron structures in laser ablated YBa₂Cu₃O_{7-x} thin films, PhD Thesis, Chalmers University of Technology, 1999.
- [13] M.S. Raven, E.E. Inametti, Y.M. Wan, B.G. Murray, *Supercond. Sci. Technol.* 7 (1994) 462.
- [14] P.B. Mozhaev, P.V. Komissinski, N.P. Kukhta, G.A. Ovsyannikov, J.L. Skov, *J. Supercond.* 10 (3) (1997) 221.

- [15] P. Kubat, P. Engst, Z. Zelinger, J. Wild, P. Bonacek, *J. Appl. Phys.* 77 (6) (1995) 2822.
- [16] M.G. Norton, R.R. Biggers, I. Maartense, E.K. Moser, J.L. Brown, *Physica C* 233 (1994) 321.
- [17] I.E. Graboy, A.R. Kaul', Yu.G. Metlin, *Results of science and technique VINITI AS USSR, Chem. Solid State* 6 (1989) 3, in Russian.
- [18] M. Ece, E.G. Gonzalez, H.-U. Habermeier, B. Oral, *J. Appl. Phys.* 77 (4) (1995) 1646.
- [19] G. Ockenfuss, R. Wordenweber, T.A. Scherer, R. Unger, W. Jutzi, *Physica C* 243 (1-2) (1995) 24.
- [20] S.C. Tidrow, W.D. Wilber, A. Tauber, S.N. Schauer, D.W. Eckart, R.D. Finnegan, R.L. Pfeffer, *J. Mater. Res.* 10 (7) (1995) 1622.
- [21] C.T. Cheung, E. Ruckenstein, *J. Mater. Res.* 4 (1) (1989) 1.
- [22] G.L. Skofronick, A.H. Carim, S.R. Foltyn, R.E. Munechausen, *J. Appl. Phys.* 76 (8) (1994) 4753.
- [23] A.D. Mashtakov, I.M. Kotelyanskii, V.A. Lusanov, P.B. Mozhaev, G.A. Ovsyannikov, I.K. Bdikin, *Tech. Phys. Lett. Pis'ma v ZhTF* 23 (19) (1997) 8, in Russian.
- [24] D.M. Hill, H.M. Meyer, J.H. Weaver, *J. Appl. Phys.* 65 (12) (1989) 4943.